Check for updates

Enhancement of Photovoltaic Current through Dark States in Donor-Acceptor Pairs of Tungsten-Based Transition Metal Di-Chalcogenides

Sayan Roy, Zixuan Hu, Sabre Kais, and Peter Bermel*

As several photovoltaic materials experimentally approach the Shockley–Queisser limit, there has been a growing interest in unconventional materials and approaches with the potential to cross this efficiency barrier. One such candidate is dark state protection induced by the dipole–dipole interaction between molecular excited states. This phenomenon has been shown to significantly reduce carrier recombination rate and enhance photon-to-current conversion, in elementary models consisting of few interacting chromophore centers. Atomically thin 2D transition metal di-chalcogenides (TMDCs) have shown great potential for use as ultra-thin photovoltaic materials in solar cells due to their favorable photon absorption and electronic transport properties. TMDC alloys exhibit tunable direct bandgaps and significant dipole moments. In this work, the dark state protection mechanism has been introduced to a TMDC based photovoltaic system with pure tungsten diselenide (WSe_2) as the acceptor material and the TMDC alloy tungsten sulfo-selenide (WSeS) as the donor material. Our numerical model demonstrates the first application of the dark state protection mechanism to a photovoltaic material with a photon current enhancement of up to 35% and an ideal photon-to-current efficiency exceeding the Shockley–Queisser limit.

1. Introduction

Since its discovery in the 1960s, the Shockley–Queisser (S–Q) efficiency limit has generally been viewed as a fundamental limit on the performance of conventional photovoltaic devices[1,2] because the detailed balance principle defines a non-trivial loss associated with the radiative recombination process.

S. Roy, Prof. P. Bermel
Department of Electrical and Computer Engineering
and Birck Nanotechnology Center
Purdue University
West Lafayette, IN 47907, USA
E-mail: pbermel@purdue.edu
Dr. Z. Hu, Prof. S. Kais
Department of Chemistry
Department of Physics, and Purdue Quantum Science
and Engineering Institute
Purdue University
West Lafayette, IN 47907, USA

The ORCID identification number(s) for the author(s) of this article can be found under https://doi.org/10.1002/adfm.202100387.

After decades of progress, recent work has brought certain high-performance photovoltaics made from multiple materials within several percent of this limit.[3] Solar cells have been shown to exhibit strong internal and external luminescence as they approach the S–Q limit, which limits their maximum efficiencies.[4] Concentrators are the most straightforward approach to increase the S–Q efficiency, but generally require operating at high temperatures, or with large cooling structures, and have not been widely adopted commercially.[5] Solar cells composed of nanophotonic structures have also been widely studied to help extend the S–Q limit (e.g., by restricting the range of incident angles for increased open circuit voltage), but current experimental devices have significant limitations in achieving higher efficiencies and stability.[6–8] As a result of these constraints, there has been a growing interest in many unconventional materials and approaches with the potential to break the S–Q limit.[9,10]

Arguably, the most successful approach is multijunction photovoltaics, where the solar spectrum is split by stacking materials with different bandgaps.[11] However, the cost of publicly known fabrication approaches can be orders of magnitude higher than single junctions.[12] In a related approach, multiple spectrum solar cells transform the broad solar spectrum to a narrow range of photon energies, such as in thermophotovoltaics;[13] however, a major challenge is in obtaining higher efficiency devices. Multiple absorption is a mechanism where a single, high-energy photon generates multiple electron-hole pairs for higher efficiencies,[14] but there is significant difficulty in the subsequent transport and collection of carriers. Another approach to obtain increased incident energy absorption is hot carrier extraction,[15] but a major challenge is fabricating a device to efficiently extract this excess energy. It is also possible to obtain AC solar cells by treating the incident photons as electromagnetic waves, as demonstrated in optical rectennas,[16] but scaling such devices to optical frequencies is a major technical challenge. Upconversion of sub-bandgap energy photons is a novel method of absorbing incident photons which otherwise cannot be absorbed,[17] but it comes with major challenges such as long-term stability and absorption of excited photons. Another approach uses multiple

ADVANCED
SCIENCE NEWS
www.advancedsciencenews.com

ADVANCED
FUNCTIONAL
MATERIALS
www.afm-journal.de

energy levels for demonstrable increases in photon absorption, such as intermediate band solar cells[18] and quantum well solar cells.[19]

In this work, we present another approach based on multiple energy levels in our absorber. While most prior techniques use these levels to increase photon absorption, our approach does not expect increased absorption. Instead, our approach uses the newly-formed energy levels to greatly reduce carrier recombination for more efficient carrier extraction. This allows for higher photon-to-current conversion with previously demonstrated levels of photon absorption. As inspired by the Shockley–Queisser efficiency limit, a natural direction of designing high efficiency photovoltaic systems is to reduce the carrier recombination rate. To this end, recent research[20–24] has investigated the possibility of using quantum effects in chromophore complexes to improve solar cell performance.[25,26] Optically dark states created by dipole–dipole interaction between molecular excited states can reduce radiative recombination in exciton transfer, effectively increasing the photocell efficiency.[20–24,27]

Dark states have been observed across a wide range of experiments, resulting in dramatic, readily observable effects. Electromagnetically-induced transparency in atoms with 2 pairs of nearly degenerate transitions give rise to dark and light states with orders of magnitude difference in transmission through condensates of these atoms.[28] Similarly, dark states in polaritons have been observed experimentally to cause dynamic light trapping of incident light pulses.[29] Dark states can also be observed in molecular systems to give rise to unusually efficient luminescence of solid-phase emitter molecules.[30]

Recent studies[20–24] have investigated dark states created by dipole–dipole interaction between molecular exciton states in chromophore complexes, which can increase the photocell efficiency by protecting the excitation from radiative recombination.[25–27] Such interactions and the formation of stable bright and dark states are widely observed phenomena in experimental studies of pigment-protein complexes in photosynthesis and have been associated with the very high exciton capture efficiency in such processes. Although these studies point to a promising design principle for artificial photocells, they are quite limited to elementary models consisting of few interacting chromophore centers, and the dark state protection mechanism has not been applied to a specific material-based photovoltaic model. Therefore, it is the goal of the current study to investigate the possibility of creating dark states in a realistic material to enable dark state protection and increase photocell efficiency with a realistic material model to facilitate experimental realization.

In this work, we use a photovoltaic model based on transition metal di-chalcogenide (TMDC) materials to demonstrate the dark state protection mechanism's ability to enhance the photocurrent, thus getting closer to an actual material design to overcome the Shockley–Queisser limit. Our primary focus is on suppressing radiative recombination. We have investigated an ideal model where losses occur primarily through recombination from the excited state; losses from the dark state, as well as other losses, are considered to be negligible. For sufficiently high-quality materials, non-radiative loss is much smaller than radiative loss. Additionally, the Shockley–Queisser Limit is derived by considering the non-radiative loss preventable, while treating radiative losses as unavoidable, which is thermodynamically required for a two-level system without dark state protection.[31]

TMDCs have gathered an increasing amount of interest recently for photovoltaic (PV) applications[32–34] because of their promising electronic and optical properties. It is possible to obtain alloys of TMDCs by altering their composition to contain more than one kind of chalcogen atoms,[35] leading to the formation of hybrid TMDCs with tunable electronic and optical properties. Here we look at tungsten-based TMDC alloys containing sulfur and selenium, whose properties are intermediate of tungsten disulfide (WS_2) and tungsten diselenide (WSe_2) with tunable direct bandgaps dependent on the sulfur and selenium concentrations.

We have modelled a solar cell composed of pure tungsten diselenide (WSe_2) as the acceptor material and a TMDC alloy, tungsten sulfo-selenide (WSeS), as the donor material, in analogy with a heterojunction solar cell. For the donor, two layers of WSeS are placed on top of each other and the dipole–dipole interaction between the two layers split the conduction band into a bright band and a dark band. The dark band can then enable the dark state protection mechanism and enhance the photocurrent generated. WSeS has a large permanent dipole moment, whereas WSe_2 does not have any permanent dipole moment, thus the donor–acceptor coupling is a dipole-induced dipole interaction.

The electronic properties of WSe_2 and WSeS were studied using density functional theory (DFT) calculations, from which the band structures and corresponding bandgaps, dipole moments, and coupling energies were obtained. The exciton transfer dynamics is calculated by a model based on Pauli master equations[20,21] and the photocurrent is calculated by the standard model for photocells.[22,25,26] Our numerical model demonstrates the first application of the dark state protection mechanism to a material based photovoltaic system with a photon current enhancement of up to 35% and an ideal energy conversion efficiency exceeding the Shockley–Queisser limit.

2. Results and Discussion

2.1. Band Structure of Tungsten-Based Pure TMDCs and Alloys

We investigated alloys of TMDC alloys by altering the composition to contain more than one chalcogen atom, leading to hybrid TMDCs with tunable properties. We calculated the band structures of both pure and hybrid TMDCs by DFT calculations. The bandgaps of pure WS_2 and WSe_2 are 2.15 and 1.67 eV, respectively. For a tungsten-based TMDC alloy containing both S and Se atoms, the bandgap is an intermediate value depending on the chalcogen composition. The bandgaps of the alloys show an approximately linear decrease with increasing Se concentration from WS_2 (2.15 eV) to WSe_2 (1.67 eV) as shown in **Figure 1**. All the hybrid alloys are found to have a direct bandgap, similar to WS_2 and WSe_2.

2.2. Dipole Moment of Hybrid TMDCs

The dipole moments of WS_2 and WSe_2 are zero, since they have the same chalcogen atoms located symmetrically on both
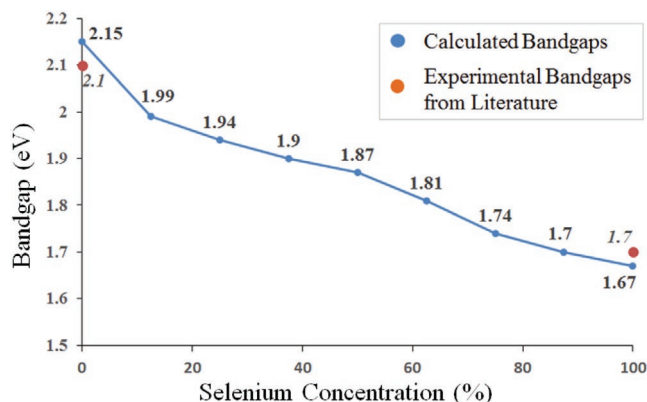
Figure 1. Variation of bandgap in a tungsten-based TMDC alloy as a function of selenium concentration and comparison to experimental bandgaps from existing literature.[36,37]

sides of the tungsten atoms. Starting from pure WS_2, the dipole moment was found to increase linearly with increasing Se concentration from 0% to 50%. For Se concentrations above 50%, the dipole moment decreased with further increase of Se concentration due to reappearance of symmetric atomic positions. Among the alloys, tungsten sulfo-selenide (WSeS) was found to have the highest dipole moment (0.27 D per molecule) since it has the most asymmetrical structure with only S atoms on one side of W atoms, and only Se atoms on the other side of W atoms.

2.3. Donor–Acceptor Photovoltaic Model

We use a donor–acceptor photovoltaic model composed of TMDC materials (**Figure 2**). The material structure model is shown in Figure 2A: WSeS with a bandgap of 1.87 eV was chosen as the donor in our system; WSe_2 with a bandgap of 1.67 eV was chosen as the acceptor, since its lower bandgap favors the band alignment of our model. The donor consists of two layers of WSeS arranged on top of each other. There is

strong dipole–dipole coupling between the two donor layers because of the large permanent dipole moment in each layer, and consequently the conduction band splits into a bright band and a dark band with an 18 meV energy gap. The induced polarization in the acceptor layer was calculated with the electric field from the donor layers (SI 3). The donor–acceptor coupling energy (γ_C) was calculated from the dipole-induced dipole interaction energy between the WSeS layers and the WSe_2 layer. For the equilibrium donor–acceptor spacing of 3 Å,[38] the coupling energy is 515 μeV, which decreases with increasing donor–acceptor separation to a value of around 50 μeV for 10 Å separation (see Section S3, Supporting Information). Radiative lifetimes of excitons in TMDCs are ≈5–17 ps,[39,40] corresponding to a recombination rate (γ_R) of 40–130 μeV. In our model, γ_R is taken as 100 μeV. The exciton generation rate in our model is simulated by a hot photon bath at 5800K.

The bright and the dark states form when there is coupling between two identical exciton states. In terms of a 2 by 2 Hamiltonian $H = \begin{pmatrix} E & J \\ J & E \end{pmatrix}$, the diagonal elements are the energy of the exciton states, and the off-diagonal elements are the coupling strength. Diagonalizing this Hamiltonian yields two eigenstates with one symmetric state (the bright state) and one anti-symmetric state (the dark state). The bright state is optically active, while the dark state is optically inactive. In this work, we have used the same principle and theory as in previous studies[20–27] and implemented them in an extended system where the donors and acceptors are 2D sheets instead of isolated molecules. As shown in Figure 2, if we consider each sheet of the double-sheet structure of the donor as a collective excitation state, then the two sheet states are coupled to each other through dipole–dipole interactions between the molecules of the sheets. Then the problem reduces to the 2×2 Hamiltonian given above, where now E is the energy of a single donor sheet, and J is the collective coupling strength between two sheets. Consequently, by this design we have created the bright-state/dark-state split on the TMDC sheets under the same principle established in the previous studies. In our calculations,
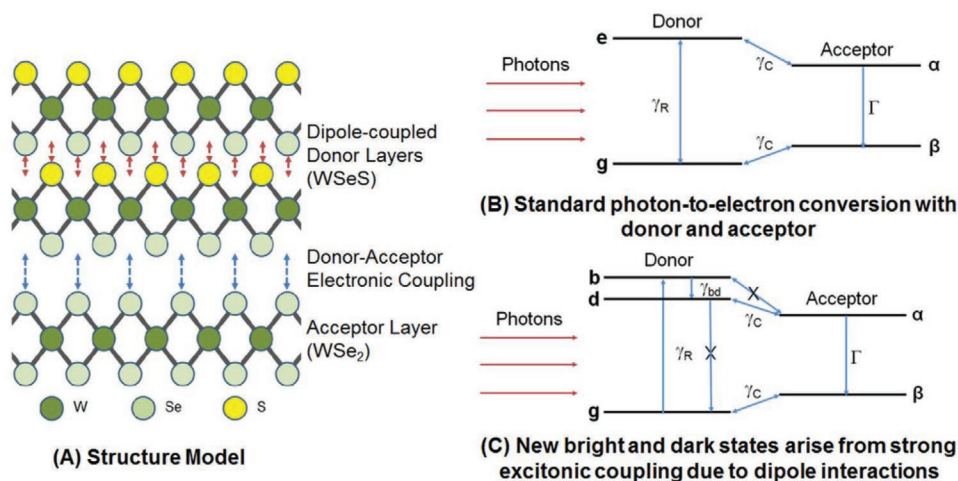

Figure 2. Donor–acceptor photovoltaic model: A) structure model; B) standard photon-to-electron conversion with donor and acceptor; and C) new bright and dark states arise from strong excitonic coupling due to dipole interactions.

we have used single unit cells of the donor and acceptor molecules to model the excitonic interactions, as in recent studies. We also used periodic boundary conditions in our calculations to account for 2D sheets of the donor and acceptor materials, so that our results are consistent for the extended system presented here.

The energy diagrams and photovoltaic dynamical models are shown in Figures 2B,C. Figure 2B shows the standard donor–acceptor model without dark state protection and Figure 2C shows the improved model with dark state protection. In both models the incoming photons generate excitations in the donor with the γ_R process, then transfer to the acceptor with the γ_C process and convert to current with the Γ process. The γ_R process is reversible, leading to the radiative recombination loss. The new additional feature of our model is the formation of new optically excitable states through strong excitonic coupling between the donor layers, as shown in Figure 2C. This leads to a splitting of the conduction band in the donor with the formation of a bright state b and a dark state d. Virtually all photonic absorption and emission takes place through the bright state. In this model, the initial absorption of photons leads to excitation on the bright state. The thermal relaxation process γ_{bd} brings the excitations from the bright state b into the dark state d where radiative recombination is forbidden. Since radiative recombination cannot occur through d, photon re-emission is suppressed and fewer excitons are lost through recombination before getting transferred to the acceptor. The excitation is then transferred from d to α. The photocurrent is determined by the rate Γ from α to β.

Any exciton generated with energy much higher than the bandgap energy will quickly undergo non-radiative (phononic) decay within the band, and then settle at the bottom of the conduction band. This phononic process is usually 1000 times faster than any optical process. In this regard, all excitons generated by photons with energies higher than the bandgap thermalize from the higher energy states to the band edge before any other process can take place. Thus, it is safe to assume that in our model, all excitons start within approximately the thermal energy kT from the bottom of the conduction band before any charge migration and harvesting can happen.

We have assumed that the donor–acceptor excitation transfer rate constant in our model is greater than or equal to the excitation rate constant from ground to the donor. Excess carriers are removed from the donor dark state by quickly transferring the excitation to the acceptor, and then to the ground, thereby completing the cycle. The dark state protection from recombination leads to an increase in the number of excitons available in the acceptor, and hence, gives a higher photocurrent in the solar cell. The overall dynamics is represented by Pauli master equations whose details can be found in Section S4, Supporting Information. Our results show that there is significant enhancement of the output photocurrent for the model in Figure 2C compared to the one in Figure 2B due to dark state protection. The current enhancement for different values of donor–acceptor separations and coupling energies are summarized in **Figure 3**.

For the equilibrium separation of 3 Å and corresponding coupling energy of 515 μeV, an enhancement of 13.4% in the output photocurrent was obtained. The current of the system without dark state protection is 4.9 mA cm^{-2}, while introducing dark state protection increases the current to 5.56 mA cm^{-2}.
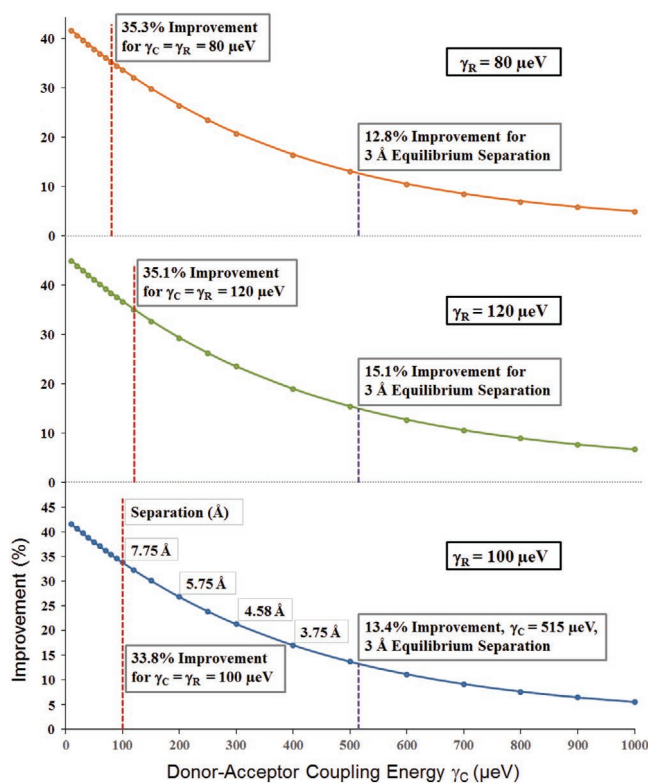

Figure 3. Improvement of output current due to dark state protection for various donor–acceptor coupling energies for $\gamma_R = 100$ μeV, and comparative performance for different values of $\gamma_R = 80$ and 120 μeV (Data taken from Roy et al.[41]).

If we look at the donor–acceptor separation scenario where the values of radiative recombination rate (γ_R) and donor–acceptor coupling energy (γ_C) are comparable to each other, we obtain a larger current enhancement of around 35% with the output photocurrent jumping from 0.99 to 1.34 mA cm^{-2} due to dark state protection (for $\gamma_C = 80$ μeV). The increase in current is the result of the suppression of radiative recombination in the donor material where the photon absorption and exciton generation takes place. Figure 3 shows that for systems where the donor–acceptor coupling energy is small compared to the rate of radiative recombination, we can obtain a greater percentage enhancement of the photocurrent by dark state protection. This is due to the competition between the donor–acceptor transfer process γ_C and the recombination process γ_R. When the donor–acceptor transfer rate is small compared to the radiative recombination rate, significant loss can occur through the recombination process unless it is suppressed by dark state protection. By implementing dipole–dipole interactions and dark state protection in our donor–acceptor model (WSeS and WSe$_2$), a current enhancement of up to 35% can be obtained.

2.4. Maximum Efficiency of Photovoltaic Model with Dark State Protection

The maximum possible efficiency of a donor–acceptor solar cell model with dark state protection was calculated (**Figure 4**) for

**ADVANCED
SCIENCE NEWS**

www.advancedsciencenews.com

**ADVANCED
FUNCTIONAL
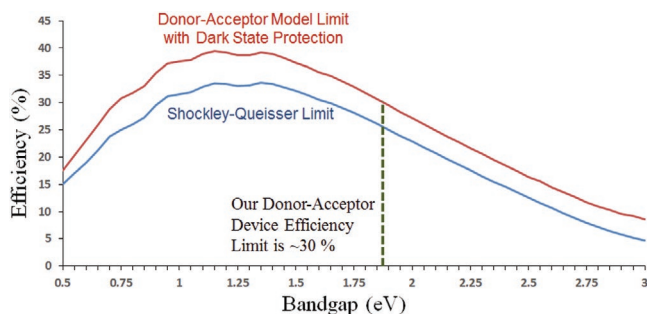MATERIALS**

www.afm-journal.de

Figure 4. Efficiency limit of a donor–acceptor photovoltaic system with dark state protection.

the AM 1.5 G spectrum[42] and compared with the well-known Shockley–Queisser limit for single junction solar cells.[1,2] It can be seen that the efficiency limit of our model is significantly higher than the Shockley–Queisser limit over the entire bandgap range of 0.5–3 eV.

Our efficiency limit calculation is an idealistic approach to evaluate the efficiency of a donor–acceptor model with perfect dark-state protection. It is assumed that all the incident photons with energies above the donor bandgap are absorbed and correspondingly excitons are generated, there is no radiative recombination in the donor (dark state protection is perfect), and there is no loss of excitons during the Γ process in the acceptor. We have accounted for carrier thermalization losses during the relaxation to the band edges in the donor and acceptor. For our donor material with bandgap 1.87 eV, we can get a maximum efficiency of around 30% using the donor–acceptor photovoltaic model with dark state protection under ideal conditions, compared to a maximum efficiency of around 26% as per the Shockley–Queisser limit for a semiconductor of the same bandgap 1.87 eV. In our model, we have overcome the detailed balance limit, but we are still within the ultimate efficiency as described by Shockley and Queisser, which is the maximum efficiency that can be achieved without radiative recombination.

The efficiency limit calculation is a purely theoretical estimation as it doesn't account for many non-idealities; dark state protection might not be perfect at room temperature or with a conduction band splitting of less than 100 meV. A major challenge is obtaining 100% photon absorption in only a few layers of the donor material. The absorption of a two-layer TMDC donor system is ≈6–7% of incident photons in the incident solar spectrum (AM 1.5), which results in the low current values in our system, consistent with experimental photovoltaic cells consisting of 2–3 layers of TMDC materials. To obtain an efficiency above the Shockley–Queisser Limit, it is necessary to add enough layers so that over 95% of the above bandgap energy photons in the incident solar spectrum could be absorbed. Also, there could be significant carrier recombination if the donor–acceptor coupling energy and the corresponding transfer rate is low, compared to the generation rate of excitons in the donor. On the other hand, if we can extract the hot carriers with energies above the band edge in the acceptor, it will lead to lower thermalization losses and allow for even higher efficiencies. Although not outright conclusive, the efficiency limit shown in Figure 4 gives an insight into the possible improvements that can be obtained with incorporating the dark state protection mechanism into a TMDC-based photovoltaic system.

3. Conclusion

We have demonstrated a TMDC-based donor–acceptor photovoltaic model, where the dark state protection mechanism is used to reduce carrier recombination and enhance photon-to-electron conversion, leading to a significantly higher current output. TMDCs have already been shown to have great potential as ultra-thin photovoltaic materials in solar cells. In this work, we have explored and modelled a heterojunction-like solar cell composed of tungsten diselenide (WSe_2) as the acceptor material and tungsten sulfo-selenide (WSeS) as the donor material. The dipole–dipole coupling between the two layers of the donor material splits the conduction band and enables the dark state protection of excitation from recombination, achieving a photocurrent enhancement as high as 35% over the standard model without dark state protection. The enhancement is more significant when the donor–acceptor transfer rate is comparable to or smaller than the recombination rate.

The principal model we present in this work exhibits the unique feature of dark state protection in an experimentally realizable system, compared to prior work on this specific topic which focused on elementary models of hypothetical molecules. While we used experimental literature values wherever possible, we did make certain assumptions about unknowns and considered the most optimistic scenarios. However, we still could expect an experimental signature of this effect across a wider range of possible parameter values, which would show up as a current enhancement compared to a control without dark state protection. For instance, even if non-radiative losses are present, the enhanced current due to dark state protection observed experimentally could be lower than that which we have modelled in this work, but it will still be higher than the system which does not have any dark state protection. The ideal values presented in this work provide an upper limit for the potential benefits of this approach, to help motivate further work in the field; importantly, experimental realization and measurement of dark state current enhancement does not require extraordinarily optimistic or even unusual parameter values.

As a potential device model for implementation, we propose a contact for hole collection on the WSeS side and a contact for electron collection on the WSe_2 side, similar to carrier collection mechanisms in the structure of heterojunction solar cells. Although a preliminary estimate, the efficiency limit of such a model has been calculated to potentially overcome the Shockley–Queisser limit if all photons above the bandgap energy are absorbed with perfect dark state protection, and there is no loss during carrier collection in the acceptor. This opens up possibilities for exploring new materials and device architectures for ultra-thin, ultra-efficient photovoltaic devices.

Our estimate of the maximum efficiency gives a possible future direction of this work, if dark state protection can be experimentally realized. It includes all the required physics in an ideal system, but does not include all non-idealities. The idealized assumptions highlight the fundamental limits of the system with dark state protection and present an upper-bound limit of the maximum possible efficiency of this system.

4. Experimental Section

Material Characterization: The band structure and corresponding bandgap, and dipole moments of pure and hybrid TMDCs were obtained by DFT calculations together with GW corrections using Quantum ESPRESSO.[43–46] TMDC alloys were investigated by altering the composition to contain more than one chalcogen atom, leading to hybrid TMDCs with tunable properties and significant dipole moments. The dipole–dipole interaction between the two donor layers (WSeS) is induced by the large permanent dipole moment in each layer. The consequent splitting of the conduction band into a bright band and a dark band with an 18 meV energy gap was obtained by DFT calculations. More details about the calculations and modelling are described in Sections S1 and S2, Supporting Information.

Donor–Acceptor Exciton Transfer Dynamics: The exciton transfer dynamics, including exciton generation from photons and corresponding output current, is represented by Pauli master equations. The details are explained in Section S4, Supporting Information.

Maximum Efficiency with Dark State Protection: The efficiency limit of a donor–acceptor solar cell model was calculated using the carrier and energy dynamics, and the incident photons in our system are taken from the data of the AM 1.5 G solar spectrum.[42] For a particular bandgap of the donor, it is assumed that all the incident photons with energies higher than the bandgap are absorbed by the donor. The excited carriers in the donor are taken as relaxed to the band edge (dark state) for current extraction and the corresponding thermalization loss is taken into account. There is additional thermalization loss during the excitation transfer from donor to acceptor since the acceptor has a lower bandgap. The output energy obtained from each carrier is the bandgap of the acceptor where the excitons decay from the excited state to the ground state, accounting for the Carnot loss.[2] The range of donor material bandgaps was taken as 0.5–3 eV, with the acceptor bandgap taken to be 0.2 eV lower than that of the donor.

$$\eta = \frac{P_{OUT}}{P_{IN}} \times 100\% \tag{1}$$

where, η – efficiency (%), P_{IN} - total input power from AM 1.5 G spectrum, P_{OUT} – output power obtained from across the acceptor material bandgap.

Any exciton generated with energy higher than the bandgap will quickly undergo non-radiative (phononic) decay within the band and then settle at the bottom of the conduction band. This phononic process is usually 1000 times faster than any optical process such that it is safe to assume all excitons start in the bottom of the conduction band before any charge migration and harvesting can happen. Consequently, the voltage is always limited by the band gap.

In the quantum heat engine model widely used by Chin, Scully, and others,[20,26] voltage is calculated to be $eV = (E_\alpha - E_\beta) - kT \ln W$, where $W = \rho_{\beta\beta}/\rho_{\alpha\alpha}$, with $\rho_{\alpha\alpha}$ being the steady state population of the acceptor's excited state, $\rho_{\beta\beta}$ the steady state population of the acceptor's ground state. eV is therefore equal to the original acceptor bandgap ($E_\alpha - E_\beta$) plus a thermodynamic correction. This makes the voltage always consistent with thermodynamics. For our system in steady state, there is no excess carrier accumulation in any of the excited states; as a result, the entropy-associated reduction in voltage is very small compared to the bandgap of the acceptor.

In a standard solar cell, there are additional voltage reductions due to the Carnot loss and the angular entropy factor from photon emission.[31] The maximum power-point voltage (V_{mp}) of a solar cell with a bandgap E_G is given by the relationship involving the Carnot factor η_C and the entropic voltage loss due to the number of arrangements W:

$$V_{mp} = E_G \, \eta_C - \frac{k_B T_c}{e} \ln(W) \tag{2}$$

where the number of arrangements $W = \frac{1}{c} \frac{\Omega_c}{\Omega_h} \frac{\rho_{\beta\beta}}{\rho_{\alpha\alpha}}$, $T_c = 300 \, K$ (room temperature), $T_h = 5800 \, K$ (temperature of the sun), and the Carnot factor

$\eta_C = 1 - T_c/T_h \approx 0.95$. The angular entropy factor is $\Delta = \frac{k_B T_c}{e} \ln\left(\frac{1}{c} \frac{\Omega_c}{\Omega_h}\right)$; it depends on the size of the solar disk (Ω_h) as viewed from the Earth, the angular radiation from the solar cell (Ω_c), and the concentration factor c (which is 1 in our case, since we are not looking at concentrated sunlight). In our model, radiative recombination is suppressed by the dark state, preventing some entropic losses. The only significant voltage reduction remaining in our system is due to the Carnot loss, which is around 5% of the bandgap energy for optimal photovoltaic materials.

Supporting Information

Supporting Information is available from the Wiley Online Library or from the author.

Conflict of Interest

The authors declare no conflict of interest.

Author Contributions

P.B. and S.K. designed the work; S.R and Z.H carried out the computations. All authors discussed the results and wrote the paper.

Data Availability Statement

The datasets generated and analyzed that support the findings of this study are available from the corresponding author upon reasonable request.

[1] W. Shockley, H. J. Queisser, *J. Appl. Phys.* **1961**, *32*, 510.
[2] L. C. Hirst, N. J. Ekins-Daukes, *Prog. Photovoltaics* **2011**, *19*, 286.
[3] M. A. Green, Y. Hishikawa, E. D. Dunlop, D. H. Levi, J. Hohl-Ebinger, A. W. Ho-Baillie, *Prog. Photovoltaics* **2019**, *27*, 3.

[4] O. D. Miller, E. Yablonovitch, S. R. Kurtz, *IEEE J. Photovoltaics* **2012**, *2*, 303.

[5] M. A. Green, S. P. Bremner, *Nat. Mater.* **2017**, *16*, 23.

[6] M. C. Beard, J. M. Luther, A. J. Nozik, *Nat. Nanotechnol.* **2014**, *9*, 951.

[7] S. A. Mann, R. R. Grote, R. M. Osgood, A. Alù, E. C. Garnett, *ACS Nano* **2016**, *10*, 8620.

[8] Y. Xu, T. Gong, J. N. Munday, *Sci. Rep.* **2015**, *5*, 13536.

[9] C. B. Honsberg, A. M. Barnett, *Eur. Photovoltaic Sol. Energy Conf.* **2005**, *20*, 453.

[10] A. Polman, M. Knight, E. C. Garnett, B. Ehrler, W. C. Sinke, *Science* **2016**, *352*, aad4424.

[11] C. H. Henry, *J. Appl. Phys.* **1980**, *51*, 4494.

[12] J. S. Ward, T. Remo, K. Horowitz, M. Woodhouse, B. Sopori, K. Vansant, P. Basore, *Prog. Photovoltaics* **2016**, *24*, 1284.

[13] Z. Zhou, E. Sakr, Y. Sun, P. Bermel, *Nanophotonics* **2016**, *5*, 1.

[14] T. Trupke, M. A. Green, P. Würfel, *J. Appl. Phys.* **2002**, *92*, 1668.

[15] D. König, K. Casalenuovo, Y. Takeda, G. Conibeer, J. F. Guillemoles, R. Patterson, L. M. Huang, M. A. Green, *Phys. E* **2010**, *42*, 2862.

[16] A. Sharma, V. Singh, T. L. Bougher, B. A. Cola, *Nat. Nanotechnol.* **2015**, *10*, 1027.

[17] S. Wen, J. Zhou, P. J. Schuck, Y. D. Suh, T. W. Schmidt, D. Jin, *Nat. Photonics* **2019**, *13*, 828.

[18] A. Luque, A. Martã, *Adv. Mater.* **2010**, *22*, 160.

[19] N. J. Ekins-Daukes, K. W. J. Barnham, J. P. Connolly, *Appl. Phys. Lett.* **1999**, *75*, 4195.

[20] C. Creatore, M. A. Parker, S. Emmott, A. W. Chin, *Phys. Rev. Lett.* **2013**, *111*, 25.

[21] Y. Zhang, S. Oh, F. H. Alharbi, G. S. Engel, S. Kais, *Phys. Chem. Chem. Phys.* **2015**, *17*, 5743.

[22] K. D. B. Higgins, B. W. Lovett, E. M. Gauger, *J. Phys. Chem. C* **2017**, *121*, 20714.

[23] Z. Hu, G. S. Engel, F. H. Alharbi, S. Kais, *J. Chem. Phys.* **2018**, *148*, 064304.

[24] Z. Hu, G. S. Engel, S. Kais, *Phys. Chem. Chem. Phys.* **2018**, *20*, 30032.

[25] M. O. Scully, *Phys. Rev. Lett.* **2010**, *104*, 20.

[26] K. E. Dorfman, D. V. Voronine, S. Mukamel, M. O. Scully, *Proc. Natl. Acad. Sci. USA* **2013**, *110*, 2746.

[27] F. H. Alharbi, S. Kais, *Renewable Sustainable Energy Rev.* **2015**, *43*, 1073.

[28] J. P. Marangos, *J. Mod. Opt.* **1998**, *45*, 471.

[29] M. D. Lukin, A. Imamoğlu, *Nature* **2001**, *413*, 273.

[30] P. Yin, Q. Wan, Y. Niu, Q. Peng, Z. Wang, Y. Li, A. Qin, Z. Shuai, B. Z. Tang, *Adv. Electron. Mater.* **2020**, *6*, 2000255.

[31] M. A. Alam, M. R. Khan, *Proc. Natl. Acad. Sci. USA* **2019**, *116*, 23966.

[32] Q. H. Wang, K. Kalantar-Zadeh, A. Kis, J. N. Coleman, M. S. Strano, *Nat. Nanotechnol.* **2012**, *7*, 699.

[33] B. Radisavljevic, A. Radenovic, J. Brivio, V. Giacometti, A. Kis, *Nat. Nanotechnol.* **2011**, *6*, 147.

[34] S. Roy, P. Bermel, *Sol. Energy Mater. Sol. Cells* **2018**, *174*, 370.

[35] Y. Gong, Z. Liu, A. R. Lupini, G. Shi, J. Lin, S. Najmaei, Z. Lin, A. L. Elías, A. Berkdemir, G. You, H. Terrones, M. Terrones, R. Vajtai, S. T. Pantelides, S. J. Pennycook, J. Lou, W. Zhou, P. M. Ajayan, *Nano Lett.* **2014**, *14*, 442.

[36] A. R. Beal, W. Y. Liang, *J. Phys. C: Solid State Phys.* **1976**, *9*, 2459.

[37] W. Zhao, Z. Ghorannevis, L. Chu, M. Toh, C. Kloc, P. H. Tan, G. Eda, *ACS Nano* **2013**, *7*, 791.

[38] J. Wilson, A. Yoffe, *Adv. Phys.* **1969**, *18*, 193.

[39] M. Palummo, M. Bernardi, J. C. Grossman, *Nano Lett.* **2015**, *15*, 2794.

[40] G. Moody, C. K. Dass, K. Hao, C. H. Chen, L. J. Li, A. Singh, K. Tran, G. Clark, X. Xu, G. Berghäuser, E. Malic, A. Knorr, X. Li, *Nat. Commun.* **2015**, *6*, 8315.

[41] S. Roy, Z. Hu, S. Kais, P. Bermel, in *PVSC*, IEEE, Chicago **2019**.

[42] Solar Spectral Irradiance: Air Mass 1.5, https://rredc.nrel.gov/solar//spectra/am1.5/ (accessed: September 2019).

[43] W. Kohn, A. D. Becke, R. G. Parr, *J. Phys. Chem.* **1996**, *100*, 12974.

[44] P. Giannozzi, S. Baroni, N. Bonini, M. Calandra, R. Car, C. Cavazzoni, D. Ceresoli, G. L. Chiarotti, M. Cococcioni, I. Dabo, A. Dal Corso, S. de Gironcoli, S. Fabris, G. Fratesi, R. Gebauer, U. Gerstmann, C. Gougoussis, A. Kokalj, M. Lazzeri, L. Martin-Samos, N. Marzari, F. Mauri, R. Mazzarello, S. Paolini, A. Pasquarello, L. Paulatto, C. Sbraccia, S. Scandolo, G. Sclauzero, A. P. Seitsonen, A. Smogunov, P. Umari, R. M. Wentzcovitch, *J. Phys.: Condens. Matter* **2009**, *21*, 395502.

[45] F. Aryasetiawan, O. Gunnarsson, *Rep. Prog. Phys.* **1998**, *61*, 237.

[46] T. Cheiwchanchamnangij, W. R. L. Lambrecht, *Phys. Rev. B* **2012**, *85*, 20.